THE JOURNAL OF PHYSICAL CHEMISTRY A
A JOURNAL OF THE AMERICAN CHEMICAL SOCIETY

pubs.acs.org/JPCA Article

Acid Gas Capture by Nitrogen Heterocycle Ring Expansion

Matthew P. Confer and David A. Dixon*

Cite This: J. Phys. Chem. A 2023, 127, 10171−10183 Read Online

ACCESS | Metrics & More | Article Recommendations | Supporting Information

ABSTRACT: Acid gases including CO_2, OCS, CS_2, and SO_2 are emitted by industrial processes such as natural gas production or power plants, leading to the formation of acid rain and contributing to global warming as greenhouse gases. An important technological challenge is to capture acid gases and transform them into useful products. The capture of CO_2, CS_2, SO_2, and OCS by ring expansion of saturated and unsaturated substituted nitrogen-strained ring heterocycles was computationally investigated at the G3(MP2) level. The effects of fluorine, methyl, and phenyl substituents on N and/or C were explored. The reactions for the capture CO_2, CS_2, SO_2, and OCS by 3- and 4-membered N-heterocycles are exothermic, whereas ring expansion reactions with 5-membered rings are thermodynamically unfavorable. Incorporation of an OCS into the ring leads to the amide product being thermodynamically favored over the thioamide. CS_2 and OCS capture reactions are more exothermic and exergonic than the corresponding CO_2 and SO_2 capture reactions due to bond dissociation enthalpy differences. Selected reaction energy barriers were calculated and correlated with the reaction thermodynamics for a given acid gas. The barriers are highest for CO_2 and OCS and lowest for CS_2 and SO_2. The ability of a ring to participate in acid gas capture via ring expansion is correlated to ring strain energy but is not wholly dependent upon it. The expanded N-heterocycles produced by acid gas capture should be polymerizable, allowing for upcycling of these materials.

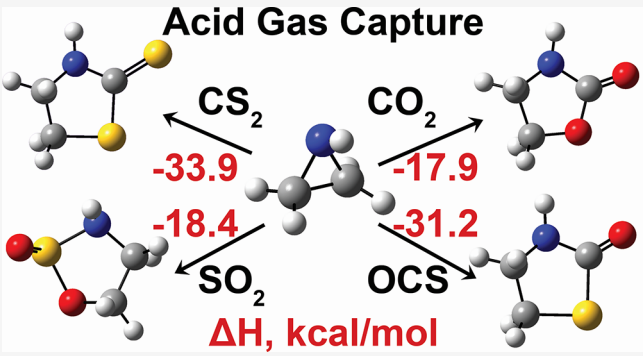

Downloaded via UNIV ILLINOIS URBANA-CHAMPAIGN on July 1, 2024 at 03:48:48 (UTC).
See https://pubs.acs.org/sharingguidelines for options on how to legitimately share published articles.

■ INTRODUCTION

Anthropogenic greenhouse gases from processes such as combustion are causing climate change due to global warming.[1−3] One possible approach to ameliorating climate impacts is to capture and convert CO_2 into products that no longer impact the atmosphere.[4−8] This would enable continued use of carbon-based fuels until energy sources that have minimal environmental impact are put into widespread production.[9−13] Amine-scrubbing by aqueous amines, primarily monoethanolamine (MEA), is a current technology for CO_2 capture, especially for CO_2 capture from the combustion of coal.[14,15] Solid-state amines for CO_2 capture from air are being developed as they are less corrosive in nature than aqueous amines and have a moderate regeneration energy.[16] CO_2 capture by aqueous amine solutions leads to the formation of carbonic acid, bicarbonate, carbamic acid, or carbamate, mostly as the respective conjugate bases due to their acidity in aqueous solution.[17−19] For example, a ^{13}C NMR study by Mani and co-workers[17] showed that H_2CO_3 formation will dominate in aqueous NH_3 solution when the amounts of NH_3 and CO_2 are comparable; however, H_2NCOOH was found to dominate when an excess of NH_3 was present. The mechanisms for the capture and conversion of CO_2 with a range of substituted amines in the gas phase and in aqueous systems has been studied using correlated molecular orbital theory with the results compared to experiment and to other computational studies.[20]

Incorporation of nitrogen into 3- and 4-membered rings, forming nitrogen heterocycles, changes the method of gas capture compared to standard amines. The ability of such N-heterocycles to trap acid gases, primarily CO_2, has been demonstrated. Experimentally, many of these reactions involved catalysts such as water and hierarchical porous silica,[21] metal organic frameworks,[22] N-heterocyclic carbenes,[23] or halide salts[24,25] or utilized supercritical CO_2[26] or ball milling.[27] Not only do such reactions trap acid gases in covalently bound molecules, but they also produce derivatives of 2-oxazolidone and 1,3-oxazinan-2-one that are synthetically valuable for both medicinal[28−30] and polymer chemistry.[31−33] A range of synthetic approaches for substituted aziridines and azetidines are available.[34−37] Aziridines are extensively used commercially in textiles, adhesives, fuels, agriculture chemicals, ion exchange resins, surfactants,[38] polymer monomers, and as alkylating agents for cancer therapy.[39,40] The use of aziridines

Received: September 10, 2023
Revised: November 5, 2023
Accepted: November 6, 2023
Published: November 22, 2023

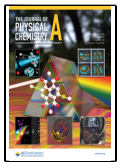

ACS Publications © 2023 American Chemical Society

https://doi.org/10.1021/acs.jpca.3c06094
J. Phys. Chem. A 2023, 127, 10171−10183

Table 1. Nitrogen Heterocycle Ring Expansion CO_2 Capture ΔH and ΔG in kcal/mol at 298 K and Exothermic to Endothermic, T_H, and Exergonic to Endergonic, T_G, Crossover Temperature between 1 and 10,000 K at the G3(MP2) and Isodesmic G3(MP2) Levels[a]

Rxn #	Reaction	ΔH	ΔG	T_H	T_G
1	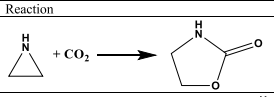	-17.9	-6.6	6772	472
2	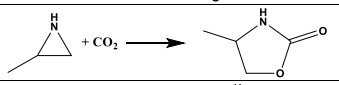	-18.1	-6.6	6795	469
3	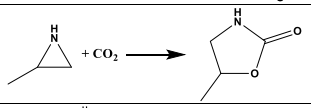	-19.3	-7.8	7193	501
4	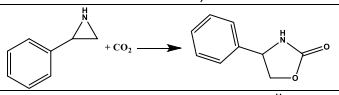	-17.5	-6.2	6590	461
5	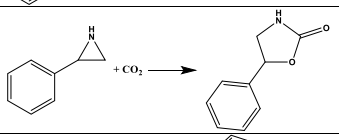	-17.4	-5.8	6563	449
6	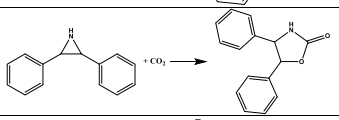	-18.2	-6.3	6802	458
7	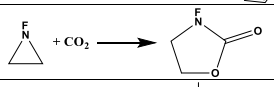	-5.1	6.5	2521	128
8	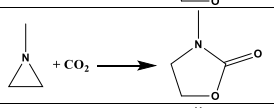	-19.3	-8.3	7310	523
9	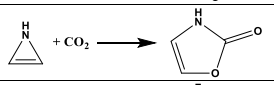	-61.3	-49.5	exo	1561
10	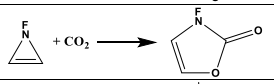	-24.5	-12.7	9217	614
11	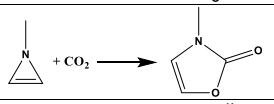	-63.0	-51.5	exo	1627
12	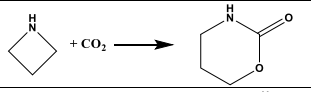	-16.3	-5.3	6161	441
13	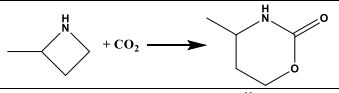	-15.7	-4.5	5949	419
14	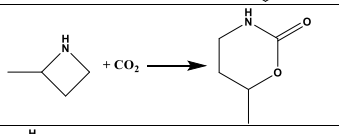	-16.8	-5.6	6306	450
15	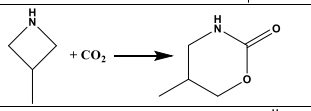	-16.3	-5.2	6152	437
16	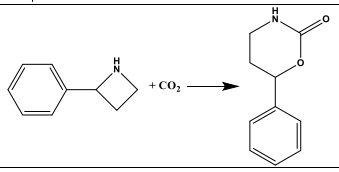	-15.2	-3.9	5748	403
17	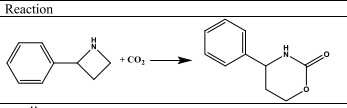	-15.0	-4.0	5660	406
18	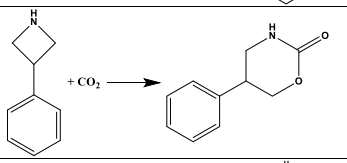	-16.1	-4.7	6101	422
19	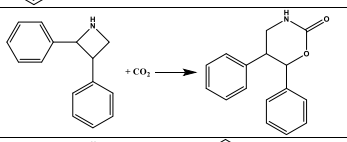	-15.1	-3.5	5712	389
20	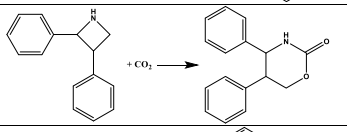	-14.7	-3.3	5548	385
21	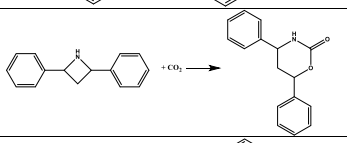	-14.7	-2.4	5559	355
22	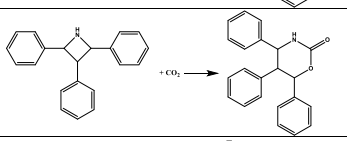	-12.8	-0.9	4774	301
23	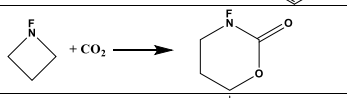	0.1	11.2	endo	ender
24	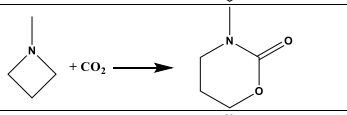	-14.3	-3.7	5565	402
25	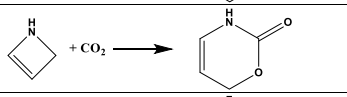	-22.0	-11.0	8127	600
26	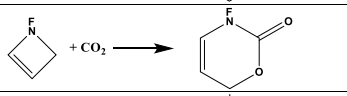	-6.5	4.8	2840	173
27	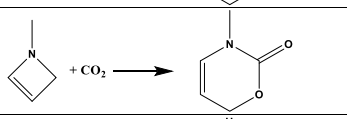	-21.5	-11.0	8014	610
28	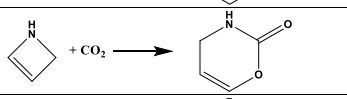	-20.3	-9.7	7594	570
29	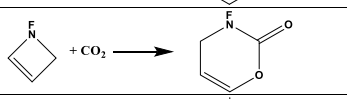	-7.5	3.9	3217	196
30	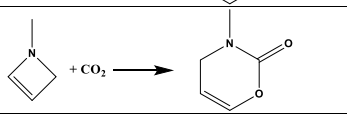	-20.4	-10.4	7659	608

[a]Isodesmic calculations with M06/DZVP2 used in place of G3(MP2) for molecules too expensive to calculate at G3(MP2).

and azetidines for novel polymerization processes has been demonstrated.[41,42] Notable aziridine containing natural products that have shown anticancer properties as DNA-alkylating and DNA cross-linking agents are the mitomycins.[43] Specifically, mitomycin C is used clinically to treat breast, esophageal, and stomach cancers.[39,44] Azetidines are com-

https://doi.org/10.1021/acs.jpca.3c06094
J. Phys. Chem. A 2023, 127, 10171−10183

monly used in medicinal chemistry,[45−49] natural products,[50−53] organic synthesis,[54,55] and organocatalysis.[56,57] Oxazolidinone based antibiotics, namely, linezolid and tedizolid, are relatively recent developments that are effective against methicillin-resistant *Staphylococcus aureus* (MRSA).[58] The oxazolidinone class of antibiotics have no cross-resistance with other antibacterial drugs due to a unique protein synthesis inhibition mechanism.[59−61]

The possibility of converting acid gas pollutants to one of the primary functional groups of currently useful antibiotics and the possibility of tractable heteroatom substitution in the oxazolidinone moiety are promising for upcycling of waste chemicals. As another example, the incorporation of oxazolidone in polymer networks has been shown to improve the mechanical toughness of self-mendable isocyanurate polymers.[32] Incorporation of phenyl substituted oxazolidone moieties into methacrylate polymers increased the glass transition temperature of the material and increase heat resistance.[31] These modified methacrylate monomers could be utilized in 3D printing applications and for dental implants.[62−65] In addition to reactions directly on isolated N-heterocycles, CO_2 insertion via ring expansion of aziridino-fullerenes has been demonstrated to proceed with a tricyclohexylphosphine catalyst.[66]

The current work extends our prior study[20] on the capture of and conversion of CO_2 by substituted amines to substituted amines with the nitrogen incorporated into a strained ring system. As strained 3- and 4-membered N-heterocycle rings are already used commercially, a goal of the current work is to show that such systems may be viable for acid gas capture; this could lead to work to further lower material costs by economy of scale. This work explores the temperature dependence as well as the solvent dependence at 298 K (THF for organic synthesis applications and water for environmental ones) thermodynamics of CO_2, OCS, CS_2, and SO_2 capture by ring expansion of N-heterocycles and investigating the relationship between ring strain energy (RSE) and reaction energetics.

■ COMPUTATIONAL METHODS

All calculations were performed with Gaussian16.[67] Molecular geometries were initially optimized at the DFT//B3LYP[68,69]/DZVP2[70] level. Vibrational frequencies were calculated to determine if the optimized geometry was a minimum or a transition state. The B3LYP/DZVP2 optimized geometries were used as the initial geometries for composite correlated G3(MP2) molecular orbital theory calculations.[71] The larger molecules were unable to be calculated at the G3(MP2) level due to the computational expense of the QCISD(T) step. Isodesmic calculations were used to minimize errors. Isodesmic calculations were benchmarked against G3(MP2) values at the DFT level using the B3LYP, ωB97XD,[72] M06,[73] PW91/PW91,[74−76] and BP86[77,78] functionals with the DZVP2 basis set using the reactions in Table S1. Benchmarking results are provided in Table S2. M06/DZVP2 values were used for isodesmic calculations, as they provided a good compromise between accuracy and computational expense. The molecules where isodesmic reactions were used and the reactions used for calculations are shown in Table S3.

Gas phase temperature dependent reaction enthalpy and free energy were calculated by determining the temperature correction to the enthalpy and entropy every 1 K from 1 to 10,000 K using Shermo.[79] Any vibrations below 100 cm^{-1} were raised to 100 cm^{-1} for the temperature dependent calculations.[80] The exothermic to endothermic transition temperature, T_H, and the exergonic to endergonic transition temperature, T_G, were calculated by determining the temperature where the reaction enthalpy and free energy, respectively, crossed 0 kcal/mol. The values "exo" or "endo" in Tables 1−4 indicate that no transition temperature was found, either because the reaction was always exothermic/exergonic or endothermic/endergonic.

Ring strain energies were calculated based upon the methods in ref 81 at the G3(MP2) level.

Single point B3LYP/DZVP2 implicit solvation calculations in tetrahydrofuran (THF) and water were performed using the self-consistent reaction field (SCRF) method[82] with SMD parameters[83] based upon B3LYP/DZVP2 geometries. These calculations yield a free energy at 298 K. An additional set of solvent calculations was performed at the SCRF level with COSMO parameters[84,85] The energies in solution were calculated as

$$\Delta G_{solution}(298\ K) = \Delta G_{gas,G3(MP2)}(298\ K) + \Delta G_{SCRF}(298\ K)$$

■ RESULTS AND DISCUSSION

CO_2 Capture. Table 1 presents thermodynamics for the capture of CO_2 by N-heterocycle reactions. Aziridine-based reactions are shown in reactions 1 to 8. At 298 K, these reactions have negative values for ΔH and except for reaction 7, 1-fluoro-aziridine, they have negative values for ΔG. Implicit solvation in THF and water at the SMD level consistently decreased the free energy change of the reaction by 4−5 kcal/mol and 6−7 kcal/mol, respectively (Supporting Information (SI) Table S4. The COSMO solvation values are within 2 kcal/mol of the SMD values on average. All aziridine-based CO_2 capture reactions are exothermic until high temperatures, but the reactions do become endergonic at the upper temperature range for flue gas (200 °C/473 K). This is due to the fact that ring expansion gas capture reactions have negative ΔS. As expected, on the basis of the thermodynamics at 298 K, the capture of CO_2 by 1-fluoro-aziridine is only exergonic at low temperatures. Addition of methyl or phenyl substituents bonded to carbon, reactions 2−3 and 4−6, respectively, did not have a dramatic change on the thermodynamics as compared to an unsubstituted aziridine. The ΔH and ΔG for aziridine and phenyl-substituted aziridines are essentially the same within the error of the method, ±1 kcal/mol, although CO_2 insertion into 2-methyl-aziridine at the γ-carbon, reaction 3, is more exothermic by 1.4 kcal/mol. Insertion of CO_2 with the phenyl group at the β-carbon is slightly more favorable than insertion at the γ-carbon whereas insertion of CO_2 into the C−N bond with the methyl group at the γ-carbon is more favorable than at the β-carbon. The most favorable aziridine-based CO_2 capture reaction occurs with 1-methyl-aziridine.

For CO_2 capture reagents, one also needs to be able to release the captured CO_2 for use in another reaction either for sequestration, for example, in the subsurface, or for use to generate useful materials. One does not want to have too high a temperature for this process to be too energy intensive but also the temperature has to be high enough for the process to occur in the capture region, for example, from flue gas.

1H-azirine based materials, reactions 9−11, are all favorable for CO_2 capture at 298 K. 1-fluoro-azirine, reaction 10, is

https://doi.org/10.1021/acs.jpca.3c06094
J. Phys. Chem. A 2023, 127, 10171−10183

Table 2. Substituted Dimethylamine CO_2 Insertion Reaction ΔH and ΔG Calculated at the G3(MP2) Level in kcal/mol and Angles at Nitrogen

Rxn #	Reaction	ΔH	ΔG	∠N Pyr React [a]	∠N Pyr Prod [a]	Σ∠X-N-X React [b]	Σ∠X-N-X Prod [b]
31	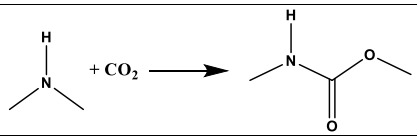	2.7	11.9	35.8	9.1	331.6	358.1
32	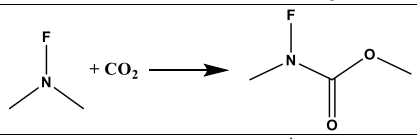	17.7	27.7	37.5	29.1	320.0	337.0
33	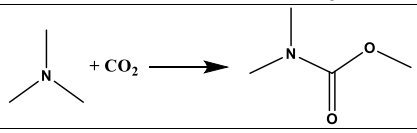	4.2	12.7	32.4	0.0	333.9	360.0

[a]Nitrogen pyramidal angle, ∠N Pyr in degrees for the reactant and product molecules, React and Prod, respectively. [b]Sum of the three nitrogen centered bond angles, Σ∠X−N−X in degrees for the reactant and product molecules, React and Prod, respectively.

dramatically less exothermic and exergonic than either azirine or 1-methyl-azirine and becomes less exergonic with implicit solvation. Although the 1H-azirine based materials have favorable CO_2 capture thermodynamics, they are generally unstable and, unless the 5-membered product ring is desired for further chemistry, are unlikely to be a feasible reagent.

CO_2 capture by azetidines, reactions 12−24, is generally favorable in both the gas phase and in THF and water (Table S4). The most favorable CO_2 capture reaction occurs with 2-methyl-azetidine, reaction 14. This reaction is favorable in the gas phase until nearly flue gas temperatures. The addition of a single methyl or phenyl substituent, reactions 13−15 and 16−18, respectively, does not have a dramatic impact on the thermodynamics. CO_2 capture by 2-phenylazetidine slightly prefers the β-carbon phenyl product to the Δ-carbon phenyl product, reactions 16 and 17, but the energetics are the same within the error of the method. 2-methyl-azetidine CO_2 capture prefers substitution at the Δ-carbon to the β-carbon by ∼1 kcal/mol in both enthalpy and free energy. CO_2 capture by 3-phenyl-azetidine is more favorable than 2-phenyl-azetidine by 0.7 kcal/mol in the gas phase but is nearly equivalent in THF, reaction 18. CO_2 based ring expansion of 2-methyl-azetidine, reaction 14, is slightly more favorable than that of 3-methyl-azetidine, reaction 15, although the results are within the error of the method. CO_2 capture by diphenyl substituted azetidine is still spontaneous but is less exergonic than by the monophenyl substituted analogs. CO_2 capture by 2,3-diphenylazetidine prefers the γ- and Δ-substituted product to the β- and γ-substituted product, reactions 19 and 20. CO_2 capture by 2,3-diphenylazetidine is more exergonic than the capture of CO_2 by 2,3-diphenylazetidine by ∼1 kcal/mol, reactions 19 and 21 respectively. CO_2 capture by 2,3,4-triphenylazetidine is only exergonic by 0.9 kcal/mol in the gas phase and becomes endergonic at 301 K, reaction 22. CO_2 capture by 1-fluoroazetidine, reaction 23, is both endothermic and endergonic at 298 K in the gas phase, remains endergonic in THF and water, and does not become spontaneous. Methyl substitution at the nitrogen, reaction 24, slightly decreases the exergonicity of the CO_2 capture but is still feasible even at temperatures near 400 K.

CO_2 capture by 2H-azetes, reactions 25−30, follows similar trends to azetidines where both unsubstituted and 1-methyl substituted systems are spontaneous and 1-fluoro substituted molecules are nonspontaneous. Unsaturation adjacent to the nitrogen, reactions 25−27, was preferential to unsaturation adjacent to the ring O, reactions 28−30, by ∼1 kcal/mol for CO_2 capture by unsubstituted and 1-methyl substituted 2H-azete whereas the opposite was preferred for 1-fluoro-2H-azete. CO_2 capture by 2H-azete and 1-methyl-2H-azete is predicted to be spontaneous past flue gas temperatures, 600 and 610 K respectively. CO_2 capture by 1-fluoro-2H-azete, unlike its saturated analogue, is predicted to spontaneous below ambient temperatures.

CO_2 capture reactions by pyrrolidines, reactions 106−123, by 2-pyrrolines, reactions 124−129, and by 3-pyrrolines, reactions 130−132 in Table S5, are all unsuitable. These reactions are both endothermic and endergonic and are nonspontaneous at any of the temperatures studied. The dramatic shift in reactivity between the 4-membered and 5-membered N-heterocycles is due to the low ring strain enthalpy (RSE) in the 5-member rings.

The effect of electron donating and withdrawing groups, independent of ring size, was tested using substituted dimethylamines, as shown in Table 2. We use these as models for fully unstrained systems. Insertion of CO_2 into dimethylamine is nearly thermoneutral and is endergonic by ∼11 kcal/mol, reaction 31, at 298 K. The dramatic shift in enthalpy and free energy of reaction caused by substitution of a strongly electron withdrawing group, fluorine, seen in the ring expansion reactions is mirrored in the insertion of CO_2 into N-fluoro-dimethylamine, reaction 32. The addition of an electron donating methyl group as represented by trimethylamine, minimally changed the thermodynamics as compared to dimethylamine driving the reaction more endothermic by 1.5 kcal/mol and endergonic by 0.8 kcal/mol, reaction 33. As expected, the addition of electron withdrawing, N-fluoro, and electron donating, *N*-methyl, substituents increased and decreased the reactant amine pyramidal angle by a small amount, respectively. Much larger changes in the amine pyramidal angle were found in the amide product, where *N*-methyl substitution allowed for a planar nitrogen (0°), a standard H substituent was slightly pyramidal (9.1°), and an N-fluoro substituent imparted a substantial pyramidal geometry (29.1°). Similar trends were found using the sum of the

https://doi.org/10.1021/acs.jpca.3c06094
J. Phys. Chem. A 2023, 127, 10171−10183

Table 3. Nitrogen Heterocycle Ring Expansion OCS Capture ΔH and ΔG in kcal/mol at 298 K and Exothermic to Endothermic, T_H, and Exergonic to Endergonic, T_G, Crossover Temperature between 1 and 10,000 K at the G3(MP2) and Isodesmic G3(MP2) Levels

Rxn #	Reaction	ΔH	ΔG	T_H	T_G
34	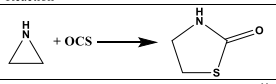	-31.2	-19.5	exo	804
35	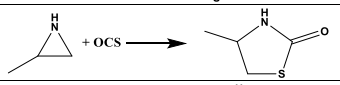	-31.3	-19.4	exo	791
36	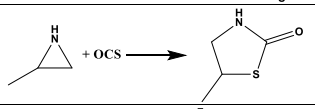	-30.2	-18.4	exo	765
37	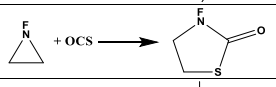	-19.3	-7.4	7201	485
38	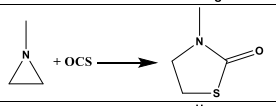	-32.8	-21.4	exo	864
39	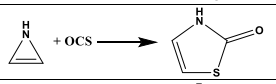	-78.3	-66.0	exo	1947
40	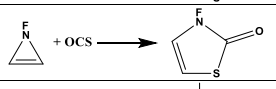	-42.8	-30.7	exo	1058
41	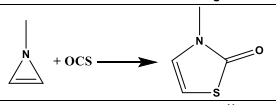	-80.1	-68.3	exo	2052
42	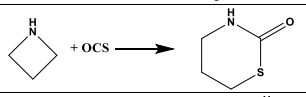	-28.3	-16.9	exo	749
43	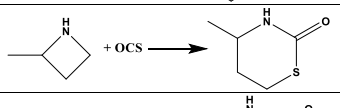	-27.6	-16.0	9824	718
44	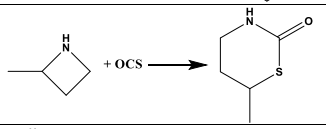	-26.7	-15.1	9550	697
45	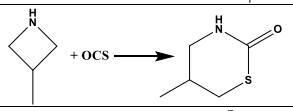	-28.3	-16.7	exo	742
46	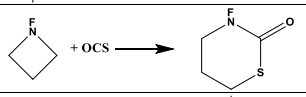	-12.2	-0.6	4649	315
47	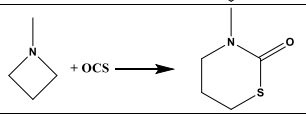	-26.1	-15.1	9448	717
48	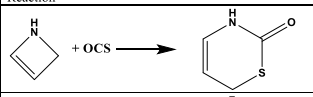	-34.7	-23.4	exo	935
49	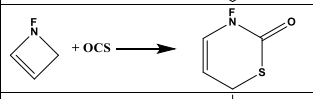	-20.0	-8.5	7262	519
50	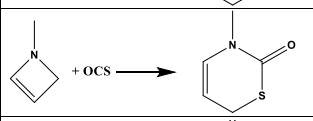	-34.2	-23.3	exo	954
51	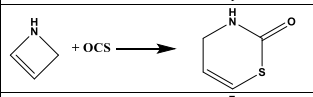	-31.6	-20.4	exo	857
52	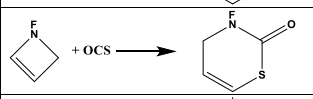	-19.6	-8.0	7185	505
53	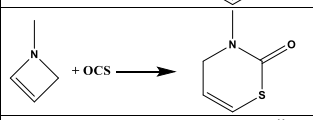	-31.7	-20.7	exo	873
54	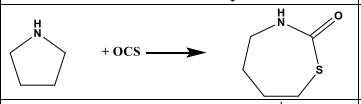	-6.3	5.7	2514	159
55		-4.2	7.7	1820	108
56	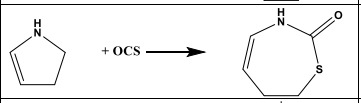	-3.6	7.7	1668	97
57	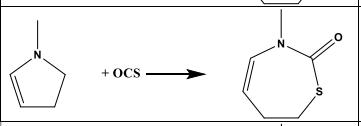	-2.1	9.3	1147	57
58	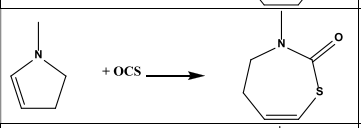	-1.3	9.8	870	37
59	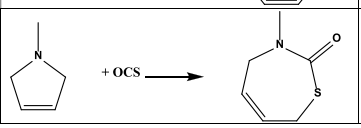	-1.7	9.4	951	48

bond angles centered upon nitrogen, where a summation of bond angles equal to 360° indicates a planar system and smaller angle summations indicate less planar, more pyramidal, systems. The planar *N*-methyl substituted product had an angle summation of 360°, as expected, whereas the slightly pyramidal unsubstituted molecule has an angle of 358.1°, and the most pyramidal product, the N-fluoro substituted molecule, has the smallest angle summation at 337.0°. The fluorine substituent on N prevents formation of a near planar > N−C(═O)- amide moiety breaking up the conjugation in the amide.

OCS Capture. OCS capture by unsubstituted, 1-fluoro-, and 1-methyl-substituted nitrogen heterocyclic ring expansion thermodynamics is presented in Table 3. OCS capture can proceed to two products: an amide or a thioamide, see reactions 34 and 133, in Table S6, respectively for examples. All thioamide product reactions are presented in Table S6. The amide geometry is preferred for all cases studied and is ∼15 kcal/mol lower in free energy than the thioamide analog regardless of ring size. This is consistent with the difference in the O═C(S) and S═C(O) bond dissociation energies (BDEs) of 159.7 ± 0.3 and 72.9 ± 0.2 kcal/mol, respectively.[86] The C−O and C−S single bonds that form are comparable in the range of 70 to 80 kcal/mol, so retention of the C═O bond is preferred. OCS capture is generally more exothermic and exergonic than the analogous CO_2 reactions due to the differences in the C═O and C═S BDEs where the O═CO BDE is 127.2 ± 0.1 kcal/mol.[86]

https://doi.org/10.1021/acs.jpca.3c06094
J. Phys. Chem. A 2023, 127, 10171−10183

Table 4. Nitrogen Heterocycle Ring Expansion CS_2 Capture ΔH and ΔG in kcal/mol at 298 K and Exothermic to Endothermic, T_H, and Exergonic to Endergonic, T_G, Crossover Temperature between 1 and 10,000 K at the G3(MP2) and Isodesmic G3(MP2) Levels

Rxn #	Reaction	ΔH	ΔG	T_H	T_G
60	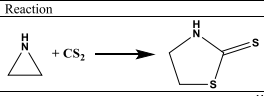	-33.9	-22.6	exo	913
61	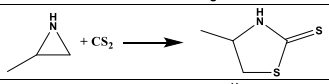	-34.0	-22.5	exo	899
62	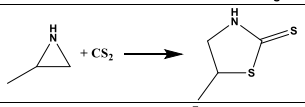	-33.2	-21.6	exo	871
63	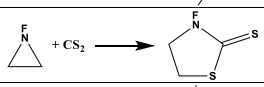	-21.4	-10.0	7870	559
64	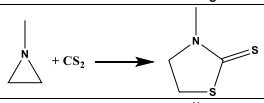	-35.9	-25.0	exo	1001
65	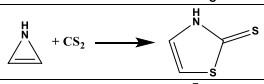	-82.9	-70.8	exo	2107
66	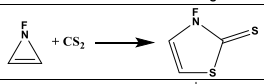	-47.9	-36.2	exo	1227
67	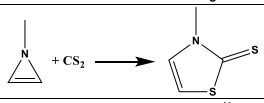	-85.8	-73.9	exo	2181
68	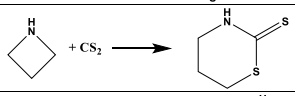	-31.5	-20.3	exo	857
69	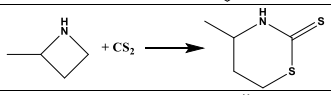	-30.8	-19.5	exo	827
70	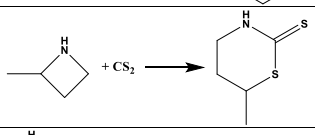	-29.9	-18.6	exo	804
71	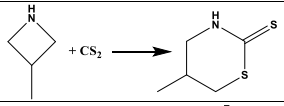	-31.5	-20.2	exo	851
72	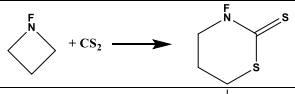	-14.4	-3.5	5363	394
73	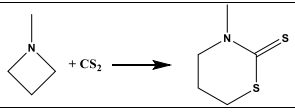	-28.9	-18.1	exo	812
74	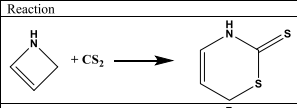	-37.9	-26.9	exo	1051
75	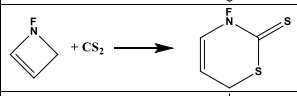	-22.5	-11.5	8097	613
76	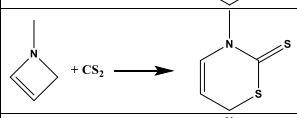	-37.2	-26.1	exo	1024
77	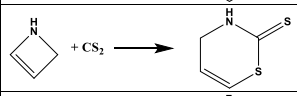	-34.6	-23.9	exo	985
78	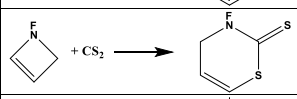	-22.1	-11.1	8005	601
79	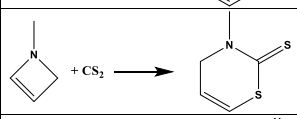	-34.9	-24.0	exo	982
80	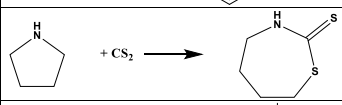	-9.3	2.4	3505	238
81	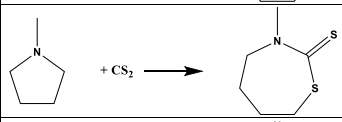	-7.3	4.4	2891	188
82	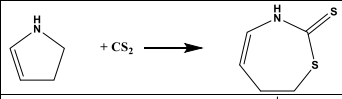	-6.1	4.9	2515	167
83	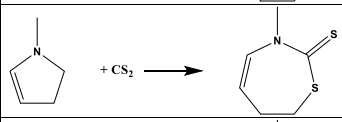	-4.0	7.2	1790	109
84	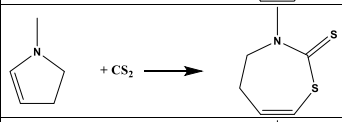	-4.4	6.7	1922	120
85	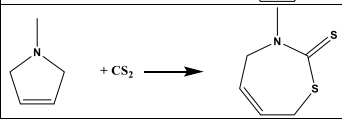	-4.9	6.0	2087	136

All aziridine based capture reactions studied, reactions 34 to 38, are spontaneous for formation of the amide and remain spontaneous past the standard maximum flue gas temperature. As with the CO_2 capture reactions, 1-fluoro-aziridine is the least spontaneous of the studied molecules and 1-methyl-aziridine is the most spontaneous. In contrast to the findings for 2-methyl-aziridine CO_2 capture, β-substitution is preferential to γ-substitution, reactions 35 and 36, respectively. 1H-azirine based OCS capture, reactions 39−41, are also all spontaneous and extremely exothermic at 298 K and remain spontaneous above experimentally relevant temperatures. The inherent limitations of 1H-azirines still remain and they are therefore unlikely to be used for OCS capture, but the resulting product rings may be interesting for polymer synthesis

All azetidines studied for the capture of OCS, reactions 42−47, are spontaneous and exothermic at 298 K and in THF or water for amide formation (Table S4). Unlike the CO_2 capture reactions, the unsubstituted and 1-methyl substituted molecules are spontaneous above standard flue gas temperatures. Unsubstituted azetidine is slightly more spontaneous than 1-methyl-aziridine, reactions 42 and 47, respectively, but at standard conditions, and even at elevated temperature, this difference is small. 1-fluoro-azetidine, reaction 46, is only slightly exergonic at 298 K, −0.6 kcal/mol, and becomes nonspontaneous just above room temperature at 315 K. In contrast to the analogous CO_2 capture reactions for 2- and 3-methyl-azetidine, γ-substitution is preferred to both β- and Δ-substitution, reactions 45, 43, and 44, respectively.

https://doi.org/10.1021/acs.jpca.3c06094
J. Phys. Chem. A 2023, 127, 10171−10183

Formation of amide products from 2H-azete OCS capture, reactions 48−53, is spontaneous until the highest accessible temperatures. In contrast to 2H-azete based CO_2 capture, the OCS capture product favors unsaturation adjacent to the nitrogen for all compounds in this study. Unsaturation adjacent to the nitrogen is favored by ∼3 kcal/mol for unsubstituted and 1-methyl-2H-azete, whereas the difference between the unsaturation location for 1-fluoro-2H-azete is 0.5 kcal/mol, which is within the error of the method. The free energy change between the unsaturation locations in 2H-azete and 1-methyl-2H-azete is greater for the OCS capture than for the CO_2 capture.

Unsubstituted, 1-methyl- and 1-fluoro-pyrrolidine, −2H-pyrroline, and −3H-pyrroline, reactions 54−59 and 153−170 in Table S6, are all nonspontaneous for OCS capture of the pyrrole at 298 K. Select molecules, including pyrrolidine, 1-methyl-pyrrolidine, 2H-pyrroline, 1-methyl-2H-pyrroline, and 1-methyl-3H-pyrroline, reactions 54−59, are spontaneous for OCS capture of the pyrrole in the gas phase at low temperatures. This low temperature spontaneity is unlikely to be experimentally relevant, as it occurs well below the dry ice-acetone bath temperature of 195 K.

CS_2 Capture. The calculated N-heterocycle ring expansion CS_2 capture reaction thermodynamics are shown in Table 4. Aziridine based CS_2 capture, reactions 60 to 64, follows trends similar to those of OCS capture. The CS_2 capture reactions are substantially more exothermic and exergonic than the analogous CO_2 and OCS reactions, and all are spontaneous until at least ∼300 °C. Similar to the OCS capture reactions, the β-substituted 2-methyl-aziridine product is favored over the γ-substituted product, reactions 61 and 62, respectively. The studied 1H-azirines, reactions 65−67, are all extremely exothermic and exergonic for CS_2 capture. 1-fluoro-1H-azirine, reaction 66, follows the same trend for CS_2 capture as for CO_2 and OCS where implicit solvation decreased the exergonicity of the reaction (Table S4). This is likely caused by implicit solvation stabilizing 1-fluoro-1H-azirine more than it stabilizes the product 5-membered ring.

CS_2 capture by the azetidines is exergonic for at 298 K, reactions 68−73, although CS_2 capture by 1-fluoro-azetidine, reaction 72, becomes nonspontaneous below standard flue gas temperatures. As with the aziridine based reactions, CS_2 capture by azetidines is both more exothermic and exergonic than the CO_2 and OCS capture reactions. Substitution preference for CS_2 capture by 2- and 3-methyl-aziridines follows the same trends as those for the OCS, and the 3-methyl-aziridine is the more spontaneous reactant, reaction 45. CS_2 capture by 2H-azetes, reactions 74−79, is spontaneous through the relevant flue gas temperature range. Similar to OCS capture and in contrast to CO_2 capture, unsaturation adjacent to the nitrogen is preferred for all species studied for CS_2 capture

CS_2 capture by ring expansion of pyrrolidines, 2H-pyrrolines, and 3H-pyrrolines, reactions 80−85 and 171−176 in Table S7, is endergonic in the gas phase at room temperature. As with OCS capture, select 5-membered rings such as pyrrolidine, 1-methyl-pyrrolidine, 2H-pyrroline, 1-methyl-2H-pyrroline, and 1-methyl-3H-pyrroline, reactions 80−85, are spontaneous or nearly spontaneous for ring expansion capture reactions at either low temperatures or in THF or water solution (Table S4).

SO_2 Capture. The thermodynamics for SO_2 capture by nitrogen heterocycles is presented in Table 5. SO_2 capture

Table 5. Nitrogen Heterocycle Ring Expansion SO_2 Capture ΔH and ΔG in kcal/mol at 298 K and Exothermic to Endothermic, T_H, and Exergonic to Endergonic, T_G, Crossover Temperature between 1 and 10,000 K at the G3(MP2) and Isodesmic G3(MP2) Levels

Rxn #	Reaction	ΔH	ΔG	T_H	T_G
86	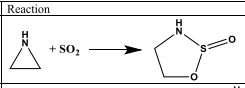	-18.4	-6.2	5132	450
87	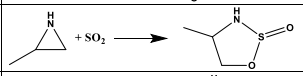	-18.2	-5.8	5076	440
88	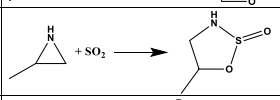	-19.3	-6.4	5371	447
89	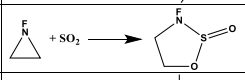	-8.1	4.4	2559	194
90	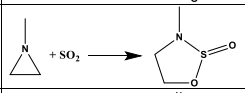	-18.9	-6.2	5320	445
91	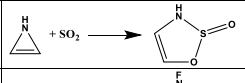	-59.2	-45.9	exo	1375
92	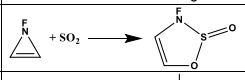	-28.8	-15.5	7894	651
93	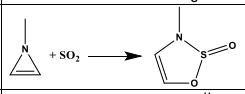	-59.3	-45.9	exo	1359
94	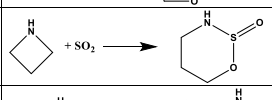	-14.6	-1.5	4112	333
95	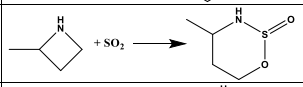	-14.2	-0.9	4006	320
96	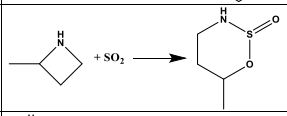	-15.1	-1.9	4238	342
97	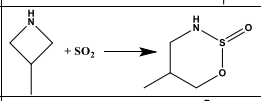	-14.6	-1.4	4105	330
98	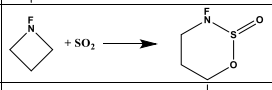	-5.4	7.7	1788	126
99	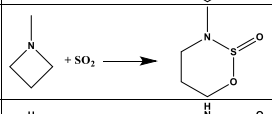	-13.0	0.2	3739	295
100	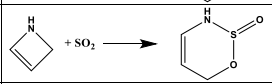	-22.6	-9.7	6169	529
101	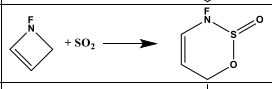	-7.7	5.2	2393	180
102	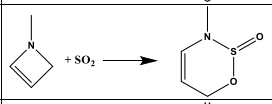	-21.8	-9.0	6002	512
103	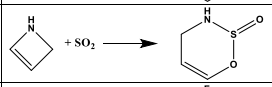	-20.9	-7.9	5756	483
104	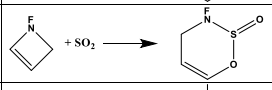	-14.4	-1.2	4079	327
105	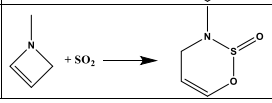	-21.2	-8.1	5831	488

https://doi.org/10.1021/acs.jpca.3c06094
J. Phys. Chem. A 2023, 127, 10171−10183

reactions are more similar to CO_2 capture reactions than to those of the OCS or CS_2 capture. This is consistent with the O═SO BDE of 131.7 kcal/mol[86] which is very similar to the O═C(O) BDE. Implicit solvation generally has a negligible effect on SO_2 capture and in many cases increases the free energy of the reaction (Table S4). This is likely due to the small free energy change upon implicit solvation of SO_2 in THF which corresponds to the relatively small Henry's Law coefficient of SO_2 in THF.[87] Implicit solvation in water does increase the exergonicity for azetidine based SO_2 capture. SO_2 capture by aziridines, reactions 86−90, is thermodynamically similar to gaseous CO_2 capture. SO_2 capture by both aziridine and 1-methyl-aziridine is spontaneous near flue gas temperatures whereas SO_2 capture by 1-fluoro-aziridine is non-spontaneous at 298 K. The free energy for SO_2 capture by 1-fluoro-aziridine increases in implicit THF solvation (Table S4) and the free energies for SO_2 capture by aziridine and 1-methyl-aziridine remain approximately constant within the error of the method. Following the trend of 2-methyl-aziridine based CO_2 capture, the γ-substituted product is favored, reaction 88. SO_2 capture by 1H-azirines, reactions 91−93, is spontaneous at 298 K with free energy changes similar in magnitude to analogous CO_2 capture reactions SO_2 capture by 1H-azirine and 1-methyl-1H-azirine is less exergonic and 1-fluoro-1H-azirine is more exergonic than the corresponding CO_2 reactions. All SO_2 capture by 1H-azirines become less exergonic in THF solution indicating that THF is not an optimal solvent for SO_2 capture by ring expansion of N-heterocycles.

SO_2 capture by azetidines, reactions 94−99, is less favorable than similar CO_2 capture reactions. Azetidine, 1-methyl, 2-methyl, and 3-methyl-azetitdine have more positive free energy changes for SO_2 than for CO_2, but 1-fluoro-azetidine becomes less endergonic compared to the analogous CO_2 reaction. The use of the studied azetidines for SO_2 capture at elevated temperatures is unlikely, but further modification to the azetidine framework may result in favorable SO_2 capture at flue gas temperatures. Analogous to CO_2 capture, 2-methyl-azetidine is slightly preferred to 3-methyl-azetidine, and the Δ-substituted product is very slightly preferred, reaction 96. SO_2 capture by 2H-azetes, reactions 100−105, is feasible at 298 K for all three compounds and at flue gas temperatures for unsubstituted 2H-azete and 1-methyl-2H-azete. Similar to CO_2 and unlike the cases of the OCS and CS_2 capture reactions, unsaturation adjacent to the nitrogen is preferred for 2H-azete and 1-methyl-2H-azete, reactions 100 and 102, but unsaturation adjacent to the oxygen is preferred for 1-fluoro-2H-azete, reaction 104, for SO_2 capture. None of the 5-membered N-heterocycles studied are feasible for SO_2 capture at any temperature or in implicit solvation, reactions 177−188 in Tables S4 and S8.

Acid Gas Association Thermodynamics and Ring Expansion Barriers. The thermodynamics for acid gas association (GA) reactions are given in the Supporting Information, Table S9. Formation of an association complex between the acid gas and the amine is weakly exothermic for CO_2, CS_2, and OCS but endergonic due to complex formation from two particles to one (see Supporting Information). Complex formation for the addition of SO_2 to an amine is substantially more exothermic, and the free energies of complex formation are all near 0 kcal/mol or are slightly negative.

The ring expansion reaction energy barriers for select 3- and 4-membered saturated rings are presented in Table 6 with a representative reaction free energy pathway presented in Figure 1. The reaction thermodynamics are consistent with previously reported values for CO_2 capture by 1,2-dimethyl-azirdine, ΔG (initial complex) = 3.4 kcal/mol and $\Delta G^{\ddagger}$ (ring expansion energy barrier from complex) = 51.7 kcal/mol (see Table 6 and Supporting Information).[22] Ring expansion reaction energy barriers are substantial and indicate that

Table 6. Acid Gas Capture Ring Expansion Pathway Barrier $\Delta H^{\ddagger}$ and $\Delta G^{\ddagger}$ in kcal/mol at the G3(MP2) Level

ring	Rxn #	$\Delta H^{\ddagger}$	$\Delta G^{\ddagger}$
	CO_2		
aziridine	1	55.4	66.3
2-methyl-aziridine	2	54.2	65.3
2-methyl-aziridine	3	51.4	62.2
1-fluoro-aziridine	7	62.4	73.5
1-methyl-aziridine	8	51.4	62.1
azetidine	12	58.3	69.2
2-methyl-azetidine	13	57.9	69.0
2-methyl-azetidine	14	55.3	66.1
3-methyl-azetidine	15	58.3	69.2
1-fluoro-azetidine	23	63.1	74.2
1-methyl-azetidine	24	56.1	67.1
	OCS		
aziridine	34	49.2	60.4
2-methyl-aziridine	35	48.4	59.9
2-methyl-aziridine	36	45.8	56.9
1-fluoro-aziridine	37	55.3	66.8
1-methyl-aziridine	38	45.9	57.1
azetidine	42	53.2	64.4
2-methyl-azetidine	43	52.7	64.1
2-methyl-azetidine	44	50.3	60.9
3-methyl-azetidine	45	53.1	64.3
1-fluoro-azetidine	46	57.2	68.4
1-methyl-azetidine	47	50.7	62.0
	CS_2		
aziridine	60	43.3	54.2
2-methyl-aziridine	61	42.4	53.5
2-methyl-aziridine	62	39.8	50.5
1-fluoro-aziridine	63	52.9	64.0
1-methyl-aziridine	64	41.6	52.7
azetidine	68	47.6	58.2
2-methyl-azetidine	69	46.9	57.9
2-methyl-azetidine	70	47.4	57.9
3-methyl-azetidine	71	49.7	60.4
1-fluoro-azetidine	72	53.2	64.0
1-methyl-azetidine	73	45.1	56.1
	SO_2		
aziridine	86	43.3	55.5
2-methyl-aziridine	87	39.1	51.8
2-methyl-aziridine	88	35.0	47.6
1-fluoro-aziridine	89	45.5	57.9
1-methyl-aziridine	90	41.2	53.4
azetidine	94	43.1	55.7
2-methyl-azetidine	95	44.1	56.8
2-methyl-azetidine	96	41.5	53.5
3-methyl-azetidine	97	45.0	57.6
1-fluoro-azetidine	98	49.2	61.6
1-methyl-azetidine	99	42.1	54.7

https://doi.org/10.1021/acs.jpca.3c06094
J. Phys. Chem. A 2023, 127, 10171−10183

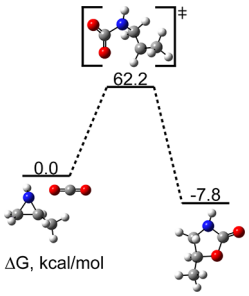

Figure 1. Reaction free energy pathway for CO_2 capture by 2-methyl-aziridine calculated at G3(MP2).

higher temperatures, such as those in flue gases or the use of catalysts, are likely necessary for this system to be experimentally useful for acid gas capture. The barriers fall in the following ranges: CO_2, 50−65 kcal/mol; OCS, 45−50 kcal/mol; CS_2, 40−55 kcal/mol; and SO_2, 35−50 kcal/mol, so SO_2 capture will have the lowest energy barriers in general. The lower barriers for SO_2 addition are in part due to the fact that SO_2 is bent, whereas the other three acid gases are linear and will have to undergo more angular distortion for the insertion reaction to occur. The barriers follow the general trends for overall reaction thermodynamics where the 1-fluoro substituted molecules are less favorable. Methyl substitution next to the ring expansion heteroatom (i.e., the γ-substituted 2-methyl-aziridine product and the Δ-substituted 2-methyl-azetidine product) consistently has a lower free energy barrier no matter if it is the thermodynamically preferred product. 3-membered ring expansion barriers are slightly lower than the corresponding 4-membered systems, generally by 3−5 kcal/mol. The small increase in ring expansion barriers upon switching from 3- to 4-membered rings is likely driven by the concomitant decrease in RSE so that less ring strain energy is released upon ring opening to accept the acid gas. This barrier difference is experimentally meaningful but still remains large even for the 3-membered rings.

In order to model a chain rather than a ring, insertion of CO_2 into dimethylamine, reaction 31 in Table 2, was studied with enthalpy and free energy barriers of 75.6 and 85.5 kcal/mol, respectively, at the G3(MP2) level. These barriers are approximately 20 kcal/mol higher than the ring structure indicating that the strained ring geometry reduces the barrier height.

A competing reaction for CO_2 capture in rings with NH moieties is the formation of carbamic acid derivatives.[20] Taking aziridine as a representative reaction, the thermodynamics for carbamic acid formation are unfavorable compared to ring expansion with positive enthalpy and free energy values: ΔH = 7.1 kcal/mol and ΔG = 16.9 kcal/mol, respectively. The reaction energy barriers, $\Delta H^{\ddagger}$ = 36.0 kcal/mol and $\Delta G^{\ddagger}$ = 46.8 kcal/mol, are smaller than that of ring expansion at the G3(MP2) level. Formation of the aziridine carbamic acid derivative is slightly less endothermic and endergonic than formation of carbamic acid from NH_3 and CO_2 with ΔH = 9.7 kcal/mol and ΔG = 18.9 kcal/mol, and has lower energy barriers as compared to $\Delta H^{\ddagger}$ = 45.1 kcal/mol and $\Delta G^{\ddagger}$ = 54.6 kcal/mol.[20] Carbamic acid formation can be catalyzed by H_2O, decreasing the enthalpy barrier by 30 kcal/mol and the free energy barrier by 12 kcal/mol.[20] The catalytic effect of H_2O on cyclic carbamic acid derivatives will be explored in future work.

Ring Strain Enthalpy. The general thermodynamics of gas capture by ring expansion of N-heterocycles is governed in part by the ring strain enthalpies (RSEs) of the reactants and products. The RSE is a measure of the increase in energy of the cyclic structure compared to reference unstrained structures; a larger RSE indicates that the ring conformation increases the energy by a greater amount. The RSE's are substantially larger for the 3- and 4-member rings than for the rings with at least 5 members. Generally, as the ring size approaches 6, the RSEs become approximately the same and near zero as they more closely resemble the angles in the unstrained analogs.

We have previously reported the RSEs for many of these species and described how to calculate them.[81] New RSEs for the reactant N-heterocycles are presented in Table 7 and the complete list is given in the SI, Table S10. Inclusion of phenyl substituents decreased the RSE with additional phenyl groups further decreasing the RSE with respect to the unsubstituted N-heterocycle. The substitution location of the phenyl moieties did not dramatically change the RSE with the largest variation being ∼1.5 kcal/mol for 3,4-diphenylpyrrolidine compared to 2,5-diphenylpyrrolidine and 2,3-diphenylpyrrolidine or 2,3,4-triphenylpyrrolidine compared to 2,3,5-triphenylpyrrolidine. The RSE variance between substitution at the 2 and 3 positions on azetidine are similar for methyl and phenyl substituents (0.9 and 1.1 kcal/mol, respectively) even though these groups have dramatically different steric effects. Additionally, the RSE values for analogous methyl and phenyl substituted systems were similar to differences <0.5 kcal/mol. For 3- and 5-membered saturated rings, the inclusion of an N-fluoro substitution increases the RSE, whereas for 4 membered rings it decreases the RSE. Inclusion of an *N*-methyl

Table 7. Ring Strain Enthalpy (RSE) of Nitrogen Heteroatom Species in kcal/mol

Molecule	RSE
2-methylaziridine	27.3
2-phenylaziridine	27.5
2,3-diphenylaziridine	28.9
1-methylaziridine	29.2
1-methyl-1H-azirene	77.8
2-methylazetidine	25.0
3-methylazetidine	25.9
2-phenylazetidine	25.2
3-phenylazetidine	26.3
2,3-diphenylazetidine	26.4
2,4-diphenylazetidine	24.1
2,3,4-triphenylazetidine	26.7
1-methylazetidine	25.4
1-methyl-1,2-dihydroazete	29.5
2-phenylpyrrolidine	6.4
3-phenylpyrrolidine	6.8
2,3-diphenylpyrrolidine	7.5
2,4-diphenylpyrrolidine	5.9
2,5-diphenylpyrrolidine	6.1
3,4-diphenylpyrrolidine	8.8
2,3,4-triphenylpyrrolidine	8.0
2,3,5-triphenylpyrrolidine	6.8
2,3,4,5-tetraphenylpyrrolidine	11.7
1-methylpyrrolidine	6.0
1-methyl-2,3-dihydropyrrole	1.9
1-methyl-2,5-dihydropyrrole	6.8

https://doi.org/10.1021/acs.jpca.3c06094
J. Phys. Chem. A 2023, 127, 10171−10183

substituent decreases the RSE in all cases except for 1H-azirine where it increases the RSE by 0.9 kcal/mol which is a minor percentage of the extremely large RSE for 1H-azirines.

The relationship between RSE and gas phase acid gas capture free energy changes is shown in Figure S1 and Table S11 for the 3- and 4-member rings. Only the amide product thermodynamics are considered for OCS capture as they are always more favorable. In the case in which a given ring can form two different products, only the most favorable reaction is used. Acid gas capture exergonicity trends with RSE depend on the ring size and saturation. The previously described trend where, for a given ring, the order of spontaneity is CS_2 > OCS > SO_2 > CO_2 is apparent in Figure S1. Overall, reasonable linear fits were found for each gas if (1) 3- and 4-membered rings were considered together, (2) if all 3-membered rings or if only the 3-membered saturated or unsaturated rings were considered, and (3) if the 3- and 4-membered unsaturated rings were grouped. Many of these reasonable linear fits are caused by the heavy dependence of ΔG on ring size due to large RSE differences between 3- and 4-membered and 5- and 6-membered rings and the large variation in RSE between unsaturated 3-membered rings. Note that the products are relatively unstrained relative to the reactants so that it is the ring strain of the reactants which is important for the 3- and 4-membered rings. Linear fits for the variance of ΔG with RSE of specific subsets comprised of saturated and unsaturated 3-membered rings and saturated and unsaturated 4-membered rings were not good. The combined 3- and 4-membered ring R^2 values are much higher than the 4-member only version because the variation in both ΔG and RSE are so heavily coupled to the size of the reactant ring. The poor fits within each ring subset are likely caused by electron donating and withdrawing substituents having different effects, or magnitudes of effect, on the RSE and ΔG. For example, the electron withdrawing properties of N-fluoro substitution consistently make acid gas capture reactions less spontaneous, whereas its effect on RSE varies depending on ring size and saturation. This is not appropriately captured by the linear fit. The 3-membered saturated rings capturing CO_2 do not follow a linear fit similar to the other acid gases. This is likely due to the increased number of rings calculated for CO_2 (the phenyl substituents) that have similar RSE but differing reaction thermodynamics. Additionally, the relatively good fits of just three-membered unsaturated rings for all gases and three-membered saturated rings for all gases except CO_2 are likely due to the low number of values in each fit (3 and 4, respectively). Linear fit equations and R^2 values for the reaction enthalpy are provided in Table S12 and generally agree with the free energy fitting results. The shortcomings of a linear fit of RSE and either ΔG or ΔH point to the need for a more complex and nuanced model. Generally, reactant rings with high strain, primarily 3- and 4-membered rings, are suitable for acid gas capture as the transition to a 5- or 6-membered product ring, respectively, releases energy as the products are not highly strained.

■ CONCLUSIONS

Acid gas capture reactions by N-heterocycle ring expansion temperature dependent thermodynamics, acid gas adsorption thermodynamics, ring expansion barrier energetics, and RSEs for phenyl- and methyl substituted N-heterocycles were studied at the G3(MP2) level. Generally, 3- and 4-membered N-heterocycles were thermodynamically favorable for acid gas capture at experimentally relevant, flue gas, temperatures due to a dramatic reduction in RSE caused by ring expansion. Inclusion of electron withdrawing nitrogen bound substituents, specifically N-fluoro, dramatically decreased the thermodynamic favorability of acid gas capture. 5-membered N-heterocycles are generally not thermodynamically suitable for acid gas capture. Capture of CS_2 and OCS was more favorable than capture of SO_2 or CO_2 due to BDE differences between C═S and C═O/S═O bonds. Acid gas adsorption at 298 K is exothermic for all N-heterocycles and gases but is exergonic only for SO_2 adsorption. Ring expansion reaction barriers are generally high, with average values of 57, 51, 46, and 42 kcal/mol for CO_2, OCS, CS_2, and SO_2, respectively. The ring expansion reaction energy barriers for 3-membered rings are slightly lower than those for the corresponding 4-membered rings. The addition of non-nitrogen bound phenyl or nitrogen bound methyl substituents generally decreased the RSE compared to the bare N-heterocycle. An increasing number of phenyl substituents further decreased the RSE, but phenyl substituent location played a minor role in the RSE. Overall, RSE and acid gas capture ΔG by ring expansion is loosely negatively correlated due to the large dependence of both values on ring size, but linear fits of RSE versus ΔG do not describe trends within a ring size well.

Acid gas capture by ring expansion of substituted N-heterocycles is a potential route to sequester greenhouse gases while, at the same time, leading to the formation of useful intermediates that can be used in the synthesis of value-added products. The inherent reactivity of the strained ring H-heterocycles increases the thermodynamic feasibility of acid gas capture and in the case of CO_2 capture leads to the formation of an amide bond. As these strained ring systems are already in use commercially as described in the Introduction, they thus may be suitable targets as acid gas capture agents.

■ ASSOCIATED CONTENT

Supporting Information

The Supporting Information is available free of charge at https://pubs.acs.org/doi/10.1021/acs.jpca.3c06094.

Complete references;[3,28,53,67] optimized Cartesian coordinates in Å; total energies; isodesmic reaction energies; endothermic reactions for 5-member rings; and implicit solvation free energies in THF and H_2O (PDF)

■ AUTHOR INFORMATION

Corresponding Author

David A. Dixon − *Department of Chemistry and Biochemistry, University of Alabama, Tuscaloosa, Alabama 35487, United States;* orcid.org/0000-0002-9492-0056; Email: dadixon@ua.edu

Author

Matthew P. Confer − *Beckman Institute for Advanced Science and Technology, University of Illinois Urbana−Champaign, Urbana, Illinois 61801, United States; Department of Chemistry and Biochemistry, University of Alabama, Tuscaloosa, Alabama 35487, United States*

Complete contact information is available at: https://pubs.acs.org/10.1021/acs.jpca.3c06094

Notes

The authors declare no competing financial interest.

https://doi.org/10.1021/acs.jpca.3c06094
J. Phys. Chem. A 2023, 127, 10171−10183

■ ACKNOWLEDGMENTS

This work was supported by UNCAGE-ME, an Energy Frontier Research Center funded by the United States Department of Energy, Office of Science, Basic Energy Sciences under Award DE-SC0012577. The EFRC is led by the Georgia Institute of Technology. D.A.D. thanks the Robert Ramsay Fund at The University of Alabama. M.P.C. acknowledges a U.S. National Science Foundation (NSF) Division of Ocean Sciences Postdoctoral Fellowship (Award Number 2205819).

■ REFERENCES

(1) Falkowski, P.; Scholes, R. J.; Boyle, E.; Canadell, J.; Canfield, D.; Elser, J.; Gruber, N.; Hibbard, K.; Högberg, P.; Linder, S.; et al. The Global Carbon Cycle: A Test of Our Knowledge of Earth as a System. *Science* **2000**, *290*, 291−296.

(2) Metz, B.; Davidson, O.; de Coninck, H.; Loos, M.; Meyer, L. (Eds.) *IPCC Special Report on Carbon Dioxide Capture and Storage*; Cambridge University Press: Cambridge, U.K., 2005; p 431.

(3) Shukla, P. R.; Skea, J.; Slade, R.; Al Khourdajie, A.; van Diemen, R.; McCollum, D.; Pathak, M.; Some, S.; Vyas, P.; Fradera, R.;et al. (Eds.) *Climate Change 2022: Mitigation of Climate Change. Contribution of Working Group III to the Sixth Assessment Report of the Intergovernmental Panel on Climate Change*. Cambridge University Press: Cambridge, UK and New York, NY, USA; 2022, p 52.

(4) Abelson, P. H. Limiting Atmospheric CO_2. *Science* **2000**, *289*, 1293.

(5) Sakakura, T.; Choi, J.-C.; Yasuda, H. Transformation of Carbon Dioxide. *Chem. Rev.* **2007**, *107*, 2365−2387.

(6) Yang, H.; Xu, Z.; Fan, M.; Gupta, R.; Slimane, R. B.; Bland, A. E.; Wright, I. Progress in Carbon Dioxide Separation and Capture: A Review. *J. Environ. Sci.* **2008**, *20*, 14−27.

(7) Hunt, A. J.; Sin, E. H. K.; Marriott, R.; Clark, J. H. Generation, Capture, and Utilization of Industrial Carbon Dioxide. *ChemSusChem* **2010**, *3*, 306−322.

(8) D'Alessandro, D. M.; Smit, B.; Long, J. R. Carbon Dioxide Capture: Prospects for New Materials. *Angew. Chem., Int. Ed.* **2010**, *49*, 625−6082.

(9) Schlapbach, L.; Züttel, A. Hydrogen-Storage Materials for Mobile Applications. *Nature* **2001**, *414*, 353−358.

(10) Coontz, R.; Hanson, B. Not So Simple. *Science* **2004**, *305*, 957.

(11) Schlapbach, L. Hydrogen-Fuelled Vehicles. *Nature* **2009**, *460*, 809−811.

(12) Kim, D. Y.; Singh, N. J.; Lee, H. M.; Kim, K. S. Hydrogen-Release Mechanism in Lithium Amidoboranes. *Chem.—Eur. J.* **2009**, *15*, 5598−5604.

(13) Kim, D. Y.; Lee, H. M.; Seo, J.; Shin, S. K.; Kim, K. S. Rules and Trends of Metal Cation Driven Hydride-Transfer Mechanisms in Metal Amidoboranes. *Phys. Chem. Chem. Phys.* **2010**, *12*, 5446−5453.

(14) Rochelle, G. T. Amine Scrubbing for CO_2 Capture. *Science* **2009**, *325*, 1652−1654.

(15) Puxty, G.; Rowland, R.; Allport, A.; Yang, Q.; Bown, M.; Burns, R.; Maeder, M.; Attalla, M. Carbon Dioxide Postcombustion Capture: A Novel Screening Study of the Carbon Dioxide Absorption Performance of 76 Amines. *Environ. Sci. Technol.* **2009**, *43*, 6427−6433.

(16) Didas, S. A.; Choi, S.; Chaikittisilp, W.; Jones, C. W. Amine−Oxide Hybrid Materials for CO_2 Capture from Ambient Air. *Acc. Chem. Res.* **2015**, *48*, 2680−2687.

(17) Mani, F.; Peruzzini, M.; Stoppioni, P. CO_2 Absorption by Aqueous NH_3 Solutions: Speciation of Ammonium Carbamate, Bicarbonate and Carbonate by a ^{13}C NMR Study. *Green Chem.* **2006**, *995*, 995−1000.

(18) Kortunov, P. V.; Siskin, M.; Baugh, L. S.; Calabro, D. C. *In Situ* Nuclear Magnetic Resonance Mechanistic Studies of Carbon Dioxide Reactions with Liquid Amines in Aqueous Systems: New Insights on Carbon Capture Reaction Pathways. *Energy Fuels* **2015**, *29*, 5919−5939.

(19) Kortunov, P. V.; Siskin, M.; Paccagnini, M.; Thomann, H. CO_2 Reaction Mechanisms with Hindered Alkanolamines: Control and Promotion of Reaction Pathways. *Energy Fuels* **2016**, *30*, 1223−1236.

(20) Lee, Z. R.; Quinn, L. J.; Jones, C. W.; Hayes, S. E.; Dixon, D. A. Predicting the Mechanism and Products of CO_2 Capture by Amines in the Presence of H_2O. *J. Phys. Chem. A* **2021**, *125*, 9802−9818.

(21) Li, Y.-N.; Xu, Q.-N.; Wu, L.-F.; Guo, Y.-H.; Yue, H.; Zhou, J.; Ge, C.-L.; Chang, H.-R. Water-Promoted Selective Cycloaddition of CO_2 and Aziridine in Confined Nanospaces of Hierarchical Porous Silica: Synergetic Effect of Chemical Function and Physical Microenvironment. *J. Environ. Chem. Eng.* **2021**, *9*, No. 105607.

(22) Zhang, C.-H.; Wu, Z.-L.; Bai, R.-X.; Hu, T.-D.; Zhao, B. Highly Efficient Conversion of Aziridines and CO_2 Catalyzed by Microporous $[Cu_{12}]$ Nanocages. *ACS Appl. Mater. Interfaces* **2023**, *15*, 1879−1890.

(23) Seayad, J.; Seayad, A. M.; Ng, J. K. P.; Chai, C. L. L. N-Heterocyclic Carbene (NHC) Catalyzed Cycloaddition of CO_2 to N-Tosyl Aziridines: Regio and Stereoselective Synthesis of Oxazolidin-2-ones. *ChemCatChem.* **2012**, *4*, 774−777.

(24) Sudo, A.; Morioka, Y.; Koizumi, E.; Sanda, F.; Endo, T. Highly efficient chemical fixation of carbon dioxide and carbon disulfide by cycloaddition to aziridine under atmospheric pressure. *Tetrahedron Lett.* **2003**, *44*, 7889−7891.

(25) Hancock, M. T.; Pinhas, A. R. A convenient and inexpensive conversion of an aziridine to an oxazolidinone. *Tetrahedron Lett.* **2003**, *44*, 5457−5460.

(26) Kawanami, H.; Ikushima, Y. Regioselectivity and selective enhancement of carbon dioxide fixation of 2-substituted aziridines to 2-oxazolidinones under supercritical conditions. *Tetrahedron Lett.* **2002**, *43*, 3841−3844.

(27) Phung, C.; Ulrich, R. M.; Ibrahim, M.; Tighe, N. T. G.; Lieberman, D. L.; Pinhas, A. R. The solvent-free and catalyst-free conversion of an aziridine to an oxazolidinone using only carbon dioxide. *Green Chem.* **2011**, *13*, 3224−3229.

(28) Xu, Z.; Tice, C. M.; Zhao, W.; Cacatian, S.; Ye, Y.-J.; Singh, S. B.; Lindblom, P.; McKeever, B. M.; Krosky, P. M.; Kruk, B. A.; et al. Structure-Based Design and Synthesis of 1,3-Oxazinan-2-one Inhibitors of 11β-Hydroxysteroid Dehydrogenase Type 1. *J. Med. Chem.* **2011**, *54*, 6050−6062.

(29) Wang, G.; Ella-Menye, J.-R.; Sharma, V. Synthesis and antibacterial activities of chiral 1,3-oxazinan-2-one derivatives. *Bioorg. Med. Chem. Lett.* **2006**, *16*, 2177−2181.

(30) Zhao, Q.; Xin, L.; Liu, Y.; Liang, C.; Li, J.; Jian, Y.; Li, H.; Shi, Z.; Lui, H.; Cao, W. Current Landscape and Future Perspective of Oxazolidinone Scaffolds Containing Antibacterial Drugs. *J. Med. Chem.* **2021**, *64*, 10557−10580.

(31) Yoshinaga, Y.; Yoshida, Y. Stereospecific radical polymerization of methacrylate bearing oxazolidone structure and improvement of glass transition temperature of urethane methacrylate copolymers. *J. Polym. Sci.* **2023**, *61*, 2050−2059.

(32) Zhang, L.; Julé, F.; Sodano, H. A. High service temperature, self-mendable thermosets networked by isocyanurate rings. *Polymer* **2017**, *114*, 249−256.

(33) Zhang, L.; Tian, X.; Malakooti, M. H.; Sodano, H. A. Novel self-healing CFRP composites with high glass transition temperatures. *Compos. Sci. Technol.* **2018**, *168*, 96−103.

(34) Degennaro, L.; Trinchera, P.; Luisi, R. Recent Advances in the Stereoselective Synthesis of Aziridines. *Chem. Rev.* **2014**, *114*, 7881−7929.

(35) Mughal, H.; Szostak, M. Recent advances in the synthesis and reactivity of azetidines: strain-driven character of the four-membered heterocycle. *Org. Biomol. Chem.* **2021**, *19*, 3274−3286.

(36) Becker, M. R.; Wearing, E. R.; Schindler, C. S. Synthesis of azetidines via visible-light-mediated intermolecular [2 + 2] photocycloadditions. *Nat. Chem.* **2020**, *12*, 898−905.

https://doi.org/10.1021/acs.jpca.3c06094
J. Phys. Chem. A 2023, 127, 10171−10183

(37) Dasi, R.; Villinger, A.; Brasholz, M. Photocatalytic Azetidine Synthesis by Aerobic Dehydrogenative [2 + 2] Cycloadditions of Amines with Alkenes. *Org. Lett.* **2022**, *24*, 8041−8046.
(38) Sommerdijk, N. A. J. M.; Buynsters, P. J. J. A.; Akdemir, H.; Geurts, D. G.; Nolte, R. J. M.; Zwanenburg, B. Aziridines as Precursors for Chiral Amide-Containing Surfactants. *J. Org. Chem.* **1997**, *62*, 4955−4960.
(39) Colvin, O. M. *Alkylating Agents. Encyclopedia of Cancer*, 2nd ed.; 2002; pp 35−42.
(40) Gad, S. C. *Ethyleneimine. Encyclopedia of Toxicology*; 3rd ed.; 2014; pp 532−534.
(41) Reisman, L.; Rowe, E. A.; Jackson, E. M.; Thomas, C.; Simone, T.; Rupar, P. A. Anionic Ring-Opening Polymerization of *N*-(tolylsulfonyl)azetidines To Produce Linear Poly(trimethylenimine) and Closed-System Block Copolymers. *J. Am. Chem. Soc.* **2018**, *140*, 15626−15630.
(42) Gleede, T.; Reisman, L.; Rieger, E.; Mbarushimana, P. C.; Rupar, P. A.; Wurm, F. R. Aziridines and azetidines: building blocks for polyamines by anionic and cationic ring-opening polymerization. *Polym. Chem.* **2019**, *10*, 3257−3283.
(43) Wolkenberg, S. E.; Boger, D. L. Mechanisms of in Situ Activation of DNA-Targeting Antitumor Agents. *Chem. Rev.* **2002**, *102*, 2477−2496.
(44) McMills, M. C.; Bergmeier, S. C. 1.02 − Aziridines and Azirines: Fused-ring Derivatives. Comprehensive Heterocyclic. *Chemistry* **2008**, *III* (1), 105−172.
(45) Kozikowski, A. P.; Tuckmantel, W.; Liao, Y.; Manev, H.; Ikonomovic, S.; Wroblewski, J. T. Synthesis and Metabotropic Receptor Activity of the Novel Rigidified Glutamate Analogues (+)- and (−)-*trans*-Azetidine-2,4-dicarboxylic Acid and Their *N*-Methyl Derivatives. *J. Med. Chem.* **1993**, *36*, 2706−2708.
(46) Burtoloso, A. C. B.; Correia, C. R. D. Stereoselective synthesis of the conformationally constrained glutamate analogue, (−)-(2R, 3S)-cis-2-carboxyazetidine-3-acetic acid, from (S)-N-tosyl-2-phenylglycine. *Synlett* **2005**, *10*, 1559−1562.
(47) Mangelinckx, S.; Boeykens, M.; Vliegen, M.; Van der Eycken, J.; De Kimpe, N. Synthesis of new 3,3-dimethoxyazetidine-2-carboxylic acid derivatives. *Tetrahedron Lett.* **2005**, *46*, 525−529.
(48) Sajjadi, Z.; Lubell, W. D. Amino acid−azetidine chimeras: synthesis of enantiopure 3-substituted azetidine-2-carboxylic acids. *J. Pept. Res.* **2005**, *65*, 298−310.
(49) Miller, R. A.; Lang, F.; Marcune, B.; Zewge, D.; Song, Z. J.; Karady, S. A practical process for the preparation of azetidine-3-carboxylic acid. *Synth. Commun.* **2003**, *33*, 3347−3353.
(50) Shioiri, T.; Irako, N.; Sakakibara, S.; Matsuura, F.; Hamada, Y. A new efficient synthesis of nicotianamine and 2-deoxymugineic acid. *Heterocycles* **1997**, *44*, 519−530.
(51) Matsuura, F.; Hamada, Y.; Shioiri, T. Total synthesis of 2′-deoxymugineic acid and nicotianamine. *Tetrahedron* **1994**, *50*, 9457−9470.
(52) Kobayashi, J.; Tsuda, M.; Cheng, J.; Ishibashi, M.; Takikawa, H.; Mori, K. Absolute stereochemistry of penaresidins A and B. *Tetrahedron Lett.* **1996**, *37*, 6775−6776.
(53) Di, Y.-T.; He, H.-P.; Wang, Y.-S.; Li, L.-B.; Lu, Y.; Gong, J.-B.; Fang, X.; Kong, N.-C.; Li, S.-L.; Zhu, H.-J.; et al. Isolation, X-ray crystallography, and computational studies of calydaphninone, a new alkaloid from Daphniphyllum calycillum. *Org. Lett.* **2007**, *9*, 1355−1358.
(54) Antermite, D.; Degennaro, L.; Luisi, R. Recent advances in the chemistry of metalated azetidines. *Org. Biomol. Chem.* **2017**, *15*, 34−50.
(55) Mehra, V.; Lumb, I.; Anand, A.; Kumar, V. Recent advances in the synthetic facets of immensely reactive azetidines. *RSC Adv.* **2017**, *7*, 45763−45783.
(56) Menguy, L.; Couty, F. Azetidine-derived bifunctional organocatalysts for Michael reactions. *Tetrahedron Asymmetry* **2010**, *21*, 2385−2389.
(57) Yoshizawa, A.; Feula, A.; Male, L.; Leach, A. G.; Fossey, J. S. Rigid and concave, 2,4-*cis*-substituted azetidine derivatives: A platform for asymmetric catalysis. *Sci. Rep.* **2018**, *8*, 6541.
(58) Lei, H.; Jiang, Y.; Wang, D.; Gong, P.; Li, Y.; Dong, Y.; Dong, M. In vitro activity of novel oxazolidinone analogs and 13 conventional antimicrobial agents against clinical isolates of Staphylococcus aureus in Beijing China. *Jpn. J. Infect. Dis.* **2014**, *67*, 402−404.
(59) Lin, A. H.; Murray, R. W.; Vidmar, T. J.; Marotti, K. R. The oxazolidinone eperezolid binds to the 50S ribosomal subunit and competes with binding of chloramphenicol and lincomycin. *Antimicrob. Agents Chemother.* **1997**, *41*, 2127−2131.
(60) Swaney, S. M.; Aoki, H.; Ganoza, M. C.; Shinabarger, D. L. The oxazolidinone linezolid inhibits initiation of protein synthesis in bacteria. *Antimicrob. Agents Chemother.* **1998**, *42*, 3251−3255.
(61) Zhou, C. C.; Swaney, S. M.; Shinabarger, D. L.; Stockman, B. J. 1H nuclear magnetic resonance study of oxazolidinone binding to bacterial ribosomes. *Antimicrob. Agents Chemother.* **2002**, *46*, 625−629.
(62) Hammer, T. J.; Shokouhi Mehr, H. M.; Pugh, C.; Soucek, M. D. Urethane methacrylate reactive diluents for UV-curable polyester powder coatings. *J. Coat. Technol. Res.* **2021**, *18*, 333−348.
(63) Patil, D. M.; Phalak, G. A.; Mhaske, S. T. Design and synthesis of bio-based UV curable PU acrylate resin from itaconic acid for coating applications. *Des. Monomers Polym.* **2017**, *20*, 269.
(64) Topa, M.; Ortyl, J. Moving Towards a Finer Way of Light-Cured Resin-Based Restorative Dental Materials: Recent Advances in Photoinitiating Systems Based on Iodonium Salts. *Materials* **2020**, *13*, 4093.
(65) Leprince, J. G.; Palin, W. M.; Hadis, M. A.; Devaux, J.; Leloup, G. Progress in dimethacrylate-based dental composite technology and curing efficiency. *Dent. Mater.* **2013**, *29*, 139−156.
(66) Takeda, Y.; Kawai, H.; Minakata, S. PCy_3-Catalyzed Ring Expansion of Aziridinofullerenes with CO_2 and Aryl Isocyanates: Evidence for a Two Consecutive Nucleophilic Substitution Pathway on the Fullerene Cage. *Eur. J. Chem.* **2013**, *19*, 13479−13483.
(67) Frisch, M. J.; Trucks, G. W.; Schlegel, H. B.; Scuseria, G. E.; Robb, M. A.; Cheeseman, J. R.; Scalmani, G.; Barone, V.; Petersson, G. A.; Nakatsuji, H.; *Gaussian 16 Rev. C.01*; Wallingford, CT, 2016.
(68) Becke, A. D. Density-functional thermochemistry. III. The role of exact exchange. *J. Chem. Phys.* **1993**, *98*, 5648−5652.
(69) Lee, C.; Yang, W.; Parr, R. G. Accurate and Simple Analytic Representation of the Electron-Gas Correlation Energy. *Phys. Rev. B* **1988**, *37*, 785−789.
(70) Godbout, N.; Salahub, D. R.; Andzelm, J.; Wimmer, E. Optimization of Gaussian-type basis sets for local spin density functional calculations. Part I. Boron through neon, optimization technique and validation. *Can. J. Chem.* **1992**, *70*, 560−571.
(71) Curtiss, L. A.; Redfern, P. C.; Raghavachari, K.; Rassolov, V.; Pople, J. A. *J. Chem. Phys.* **1999**, *110*, 4703−4709.
(72) Chai, J.-D.; Head-Gordon, M. Long-range corrected hybrid density functionals with damped atom−atom dispersion corrections. *Phys. Chem. Chem. Phys.* **2008**, *10*, 6615−6620.
(73) Zhao, Y.; Truhlar, D. G. The M06 suite of density functionals for main group thermochemistry, thermochemical kinetics, noncovalent interactions, excited states, and transition elements: two new functionals and systematic testing of four M06-class functionals and 12 other functionals. *Theor. Chem. Acc.* **2008**, *120*, 215−241.
(74) Perdew, J. P.; Wang, Y. Accurate and simple analytic representation of the electron-gas correlation energy. *Phys. Rev. B* **1992**, *45*, 13244−13249.
(75) Perdew, J. P.; Chevary, J. A.; Vosko, S. H.; Jackson, K. A.; Pederson, M. R.; Singh, D. J.; Fiolhais, C. Atoms, molecules, solids, and surfaces: Applications of the generalized gradient approximation for exchange and correlation. *Phys. Rev. B* **1992**, *46*, 6671−6687.
(76) Perdew, J. P.; Chevary, J. A.; Vosko, S. H.; Jackson, K. A.; Pederson, M. R.; Singh, D. J.; Fiolhais, C. Erratum: Atoms, molecules, solids, and surfaces: Applications of the generalized gradient

approximation for exchange and correlation. *Phys. Rev. B* **1993**, *48*, 4978−4978.
(77) Becke, A. D. Density-functional exchange-energy approximation with correct asymptotic behavior. *Phys. Rev. A* **1988**, *38*, 3098−3100.
(78) Perdew, J. P. Density-functional approximation for the correlation energy of the inhomogeneous electron gas. *Phys. Rev. B* **1986**, *33*, 8822−8824.
(79) Lu, T.; Chen, Q. Shermo: A general code for calculating molecular thermodynamic properties. *Comput. Theor. Chem.* **2021**, *1200*, No. 113249.
(80) Ribeiro, R. F.; Marenich, A. V.; Cramer, C. J.; Truhlar, D. G. Use of Solution-Phase Vibrational Frequencies in Continuum Models for the Free Energy of Solvation*J. Phys. Chem. B* **2011**, *115*, 14556−14562.
(81) Confer, M. P.; Qu, T.; Rupar, P. A.; Dixon, D. A. Composite Correlated Molecular Orbital Theory Calculations of Ring Strain for Use in Predicting Polymerization Reactions. *ChemPhysChem* **2022**, *23*, No. e202200133.
(82) Tomasi, J.; Mennucci, B.; Cammi, R. Quantum Mechanical Continuum Solvation Models. *Chem. Rev.* **2005**, *105*, 2999−3094.
(83) Marenich, A. V.; Cramer, C. J.; Truhlar, D. G. Universal Solvation Model Based on Solute Electron Density and on a Continuum Model of the Solvent Defined by the Bulk Dielectric Constant and Atomic Surface Tensions. *J. Phys. Chem. B* **2009**, *113*, 6378−6396.
(84) Klamt, A. *COSMO-RS: from quantum chemistry to fluid phase thermodynamics and drug design*; Elsevier: Amsterdam, 2005.
(85) Klamt, A.; Schüürmann, G. COSMO: a new approach to dielectric screening in solvents with explicit expressions for the screening energy and its gradient. *J. Chem. Soc., Perkin Trans.* **1993**, *2*, 799−805.
(86) Luo, Y.-R. *Comprehensive Handbook of Chemical Bond Energies*; CRC Press, Taylor and Francis Group, 2007.
(87) van Dam, M. H. H.; Lamine, A. S.; Roizard, D.; Lochon, P.; Roizard, C. Selective Sulfur Dioxide Removal Using Organic Solvents. *Ind. Eng. Chem. Res.* **1997**, *36*, 4628−4637.

https://doi.org/10.1021/acs.jpca.3c06094
J. Phys. Chem. A 2023, 127, 10171−10183